International Journal of Machine Tools & Manufacture 50 (2010) 775–788

Contents lists available at ScienceDirect

International Journal of Machine Tools & Manufacture

journal homepage: www.elsevier.com/locate/ijmactool

Pulse train data analysis to investigate the effect of machining parameters on the performance of wire electro discharge turning (WEDT) process

V. Janardhan, G.L. Samuel *

Manufacturing Engineering Section, Department of Mechanical Engineering, Indian Institute of Technology Madras, Chennai 600036, India

ARTICLE INFO

Article history:
Received 2 December 2009
Received in revised form
19 May 2010
Accepted 21 May 2010
Available online 10 June 2010

Keywords:
Wire electro discharge turning
Pulse train analysis
Material removal rate
Surface roughness
Roundness error

ABSTRACT

This paper aims at giving an insight into the wire electro discharge turning (WEDT) process, by analyzing the effect of machining parameters on material removal rate (MRR), surface roughness and roundness error, using the pulse train data acquired at the spark gap. To achieve this objective a simple and cost effective spindle is developed for the WEDT process. Pulse train data are acquired with a data acquisition system developed in the present work. A pulse discrimination algorithm has been developed for classifying the discharge pulses into open circuit, normal, arc and short circuit pulses. With the help of algorithm the number of arc regions, average ignition delay time, the width of the normal and arc regions in the data acquired can also be obtained. It has been observed that the rotation of the workpiece has significant influence on the type of the discharges occurring at the spark gap. Preliminary experiments conducted to compare the WEDM and WEDT processes disclosed that MRR is less in WEDT and the number of arcs and arc regions are more in WEDT. It has been observed that the surface roughness and roundness error of the WEDT components are influenced by the occurrence of arc regions, width of arc and normal discharge regions and average ignition delay time.

1. Introduction

The electrical discharge machining (EDM) technology has developed rapidly in the recent years and become important in precision manufacturing applications like die and mould making, micro machining, etc. Wire electrical discharge machining (WEDM) is a modified electrical discharge technique used for manufacturing components with intricate shapes and profiles, with the help of a numerically controlled travelling wire electrode. Material is eroded from the workpiece by a series of discrete sparks between the workpiece and the wire electrode (tool) separated by a thin film of dielectric fluid. Because of its wide capabilities it has applications in various fields such as automobile, aerospace, medical and virtually all areas of conductive materials machining [1]. Turning with WEDM is one of the emerging areas, developed to generate cylindrical form on hard and difficult to machine materials by adding a rotary axis to WEDM.

Several researchers have contributed to the development of the wire electrical discharge turning (WEDT). Masuzawa and Tonshoff [2] reported turning of small diameter pins of size 5 μm using WEDM. Qu et al. [3] turned automobile components like diesel injector plungers with WEDM. Takayuki et al. [4] machined arbitrary shapes on insulating ceramics. Rhoney et al. [5] trued metal bonded diamond wheels with WEDM. However the drawback of the WEDT process compared to conventional turning on lathe is that the maximum depth of cut in a single pass is limited by the wire diameter in WEDT process.

Efforts have been made to study the characteristics of the WEDT process with various machining parameters. Qu et al. [3] mathematically modeled the material removal rate (MRR), and compared MRR for WEDM and WEDT. The author observed that MRR in case of WEDT is more compared to that of WEDM. Mohammadi et al. [6] developed a mathematical relation between machining parameters on MRR using regression analysis and reported that power, voltage and servo voltage are the most significant parameters affecting the MRR and also mentioned that rotational speed and servo voltage have inverse effect on MRR. It is also mentioned that wire speed and pulse off time have no effect on MRR. Haddad and Tehrani [7] developed a mathematical relation between the machining parameters and MRR using response surface methodology and observed that power, voltage, pulse off time and rotational speed have much effect on MRR; however the pulse off time and rotational speed are reciprocally proportional to MRR.

The effect of machining parameters on surface roughness and roundness of the parts turned using WEDT is also carried out by several researchers. Qu et al. [8] developed a mathematical model for arithmetic average surface roughness in WEDT. The authors

* Corresponding author. Tel.: +91 44 22574699 (O), +91 44 22576699 (R); fax: +91 44 2257 4652.
E-mail addresses: samuelgl@iitm.ac.in, samuelgl@yahoo.com (G.L. Samuel).

0890-6955/$ - see front matter © 2010 Elsevier Ltd. All rights reserved.
doi:10.1016/j.ijmachtools.2010.05.008

Nomenclature

V_t, V_a	voltage threshold values for detecting ignition delay and non-ignition delay pulses, respectively (V)
I_t	current threshold value (A)
t_{pc}	pulse classification time interval (μs)
t_f	discharge duration (μs)
t_o	pulse off time (μs)
t_c, t_v	sampling time corresponding to current and voltage threshold crossing point (μs)
V_f	wire feed rate (mm/min)
K, **L**	sampling points in the rising direction, $\mathbf{K}=\{k_1, k_2, \ldots, K_i, \ldots, K_n\}$ prior to and $\mathbf{L}=\{l_1, l_2, \ldots, l_i, \ldots, l_n\}$ after the voltage threshold level
M, **N**	sampling points in the falling direction, $\mathbf{M}=\{m_1, m_2, \ldots, m_i, \ldots, m_n\}$ prior to and $\mathbf{N}=\{n_1, n_2, \ldots, n_i, \ldots, n_n\}$ after the voltage threshold level
O, **P**	sampling points in the rising direction, $\mathbf{O}=\{o_1, o_2, \ldots, o_i, \ldots, o_n\}$ prior to and $\mathbf{P}=\{p_1, p_2, \ldots, p_i, \ldots, p_n\}$ after the current threshold level
Q, **R**	sampling points in the falling direction, $\mathbf{Q}=\{q_1, q_2, \ldots, q_i, \ldots, q_n\}$ prior to and $\mathbf{R}=\{r_1, r_2, \ldots, r_i, \ldots, r_n\}$ after the voltage threshold level
D_1	initial diameter of the workpiece (mm)
D_2	diameter of the workpiece after machining (mm)
w	Kerf width (mm)
t	thickness of the workpiece (mm)

found that shorter pulse on time and lower feed rate created better surface finish and roundness. Haddad and Tehrani [9] modeled the surface roughness and roundness with machining parameters using response surface methodology for AISI D3 steel. The authors reported that power is directly proportional to arithmetic average surface roughness R_a, pulse off time and rotational speed have inverse effect on surface roughness parameter R_a. When the rotational speed is increased, the roundness error decreased greatly and it increased when the power and voltage are high. Mohammadi et al. [10] studied the variation in surface finish and roundness of the parts with machining parameters by developing a mathematical model using regression analysis. The authors reported that power has significant effect on surface roughness and the parameters power, wire speed and servo voltage on roundness are more significant than pulse off time, voltage and rotational speed. The MRR and surface finish depends on the discharge energy [11] and the type of the discharges occurring at the spark gap. Pulse train studies reveal typical characteristics of the discharges occurring at the spark gap [12].

Pulse train analysis includes the classification of the different types of discharges occurring at the spark gap. Several researchers have studied the classification of pulses. Dauw et al. [13] classified the discharge pulses in EDM into fifteen types with the help of voltage and time reference levels. Watanabe et al. [14] classified the discharge pulses into three categories: normal, deion and arc according to the discharge profile, to monitor and control WEDM. This method is used for offline process optimization. Yan and Liao [15] discriminated the pulses into normal and arc pulses based on ignition delay as sensing parameter to prevent wire rupture in WEDM. Liao and Woo [16] developed a pulse discriminating system to analyze the relationship between the machining settings and pulse trains in WEDM. Tarng et al. [17] classified the pulses in EDM based on the features of the measured gap voltage and gap current by using a fuzzy set theory. Yan and Chien [18] developed a computer-aided pulse discriminating and control system based on the characteristics of the gap voltage wave form.

The exact mechanism of WEDT is not reported clearly in the literature. The effect of rotational speed on roundness error reported by different researchers is not in agreement. The available literature regarding the WEDT mainly deals with studying the effect of machining parameters with the help of statistical methods and mathematical models but the same was not studied with respect to pulse trains. It is useful in providing a clear description about the variation in discharges occurring by the rotation of the workpiece and to study the effect of machining parameters on MRR, surface roughness and roundness error. To study the performance of WEDT process with pulse trains a pulse discrimination method for offline analysis is required. Most of the pulse discrimination methods discussed in the literature are used for online control of the EDM and WEDM process.

In the present work a cost effective spindle is fabricated to meet the requirements of the WEDT process. The pulse train data is collected with the help of a pulse train data acquisition system developed. A pulse discrimination algorithm has been proposed based on the voltage, current and time data obtained from data acquisition system. With the pulse discrimination algorithm the pulses are classified into four types: open, normal (spark), arc and short circuit pulses for off-line analysis of the WEDT characteristics. The effect of machining parameters such as pulse off-time, spark gap, servo feed, rotational speed and flushing pressure on MRR, surface roughness and roundness error is studied using pulse train data analysis.

2. Development of WEDT spindle

The purpose of spindle is to give rotary motion to the workpiece during discharge. Precision spindle is the key subsystem for cylindrical wire electro discharge turning process. Following are the basic requirements for the spindle:

- *Protection from flushing.*
- *High current electrical connectivity to the ground.*
- *Spindle rotational accuracy.*
- *Work holding and flexibility.*
- *Electrical insulation to the bearings*: The bearing balls and races may get eroded during the discharge due to the small clearance between them [5]. This will affect the rotational accuracy of the bearings.

Detailed explanation regarding each requirement is also available in [3].

The spindle has been fabricated to meet the requirements mentioned earlier and with a minimum cost. The cross sectional view of the bearing assembly is shown in Fig. 1(a). A straight shank ER11 collet adaptor had been modified and used as spindle shaft as shown in Fig. 1(a). The collet is locked with a nut as shown in Fig. 1(a). Generally electrical insulation to the bearings is achieved by using ceramic ball bearings. However these bearings are expensive; in the present work two sleeves made of nylon are press fit into the spindle shaft and stainless steel deep groove ball bearings are inserted over them as shown in Fig. 1(a). The housing is also made of nylon to provide electrical insulation

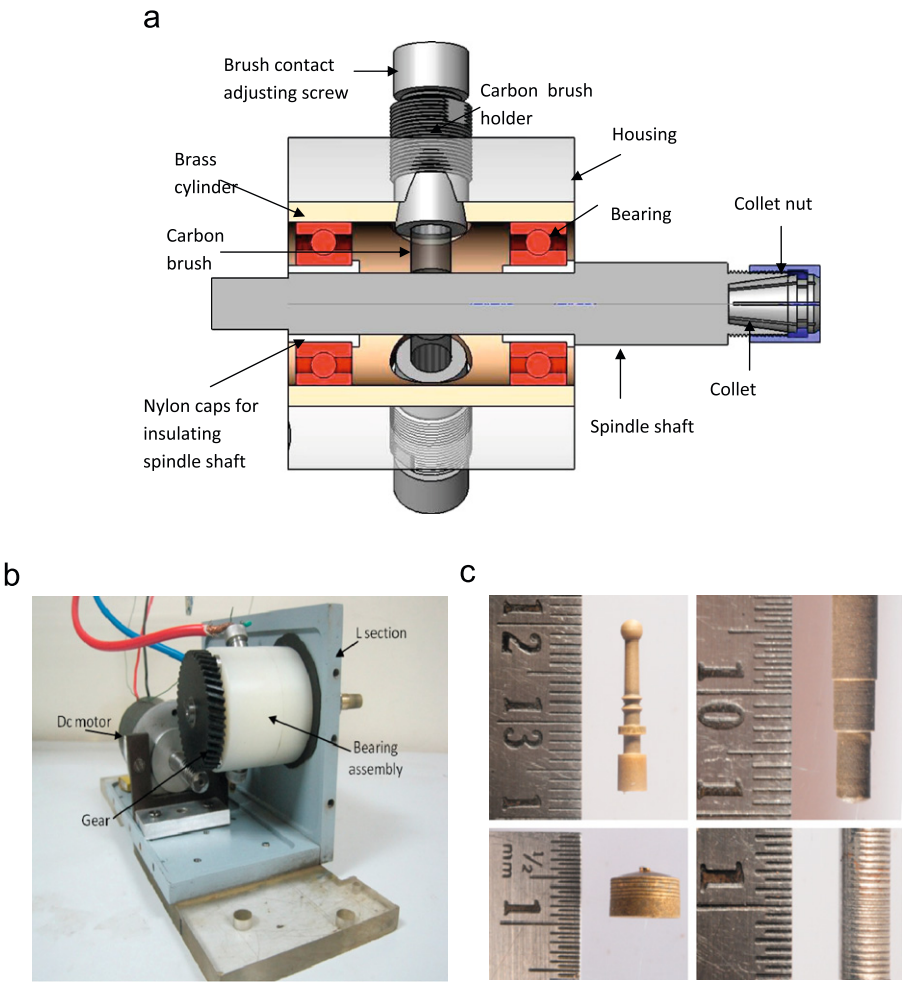

Fig. 1. Spindle for WEDT process: (a) cross sectional view of the bearing assembly, (b) spindle assembly and (c) components machined with the present setup.

to the bearings. Brass cylinder is inserted into the housing, to avoid damage of housing bore during the installation of bearings and to improve rotational accuracy. Housing is provided with threaded holes along its circumference for inserting carbon brush holder as shown in Fig. 1(a), and brush contact with the spindle shaft is adjusted with a screw as shown in Fig. 1(a). The real model of the spindle after assembling all the individual components is shown in Fig. 1(b). Both the spindle shaft and the motor shaft are connected by a Worm gear made of plastic for insulation. The bearing assembly is fixed to the vertical face of the L-section. The motor is fixed to the base of the L-section. The total spindle is covered with a casing made of acrylic plates to protect from flushing. The runout of the spindle is checked using capacitance sensor and is found to be 5 μm on the spindle shaft. Components machined with the present spindle are shown in Fig. 1(c).

3. Analysis of pulse train data

3.1. Pulse train data acquisition

Pulse train data include voltage and current waveforms across the spark gap during machining. The variation in the discharges occurring at the spark gap due to addition of rotary axis is studied using pulse train analysis. A block diagram of pulse train data acquisition system to obtain the spark gap voltage and current waveform is shown in Fig. 2. Current waveform is obtained by measuring the voltage drop across 75 mV/75 A shunt (resistance 1 mΩ). The idea of using electrical shunt for measuring gap current is reported by Murthy and Philip [19] and Gangadhar et al. [12]. Cathode ray oscilloscope is used to acquire voltage and current waveforms. Pulse train data are collected during the machining for a duration of 100 ms at different parameter settings. Voltage and current pulse train data representing different pulse types are shown in Fig. 3.

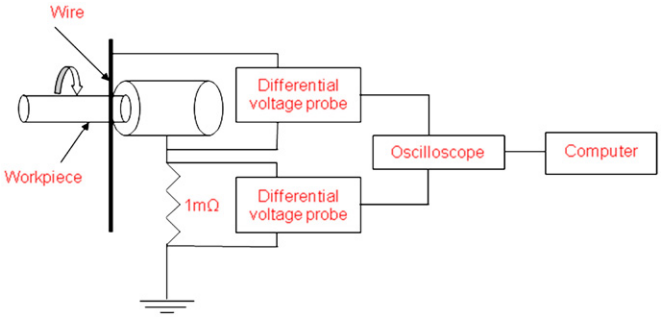

Fig. 2. Block diagram of the pulse train data acquisition system.

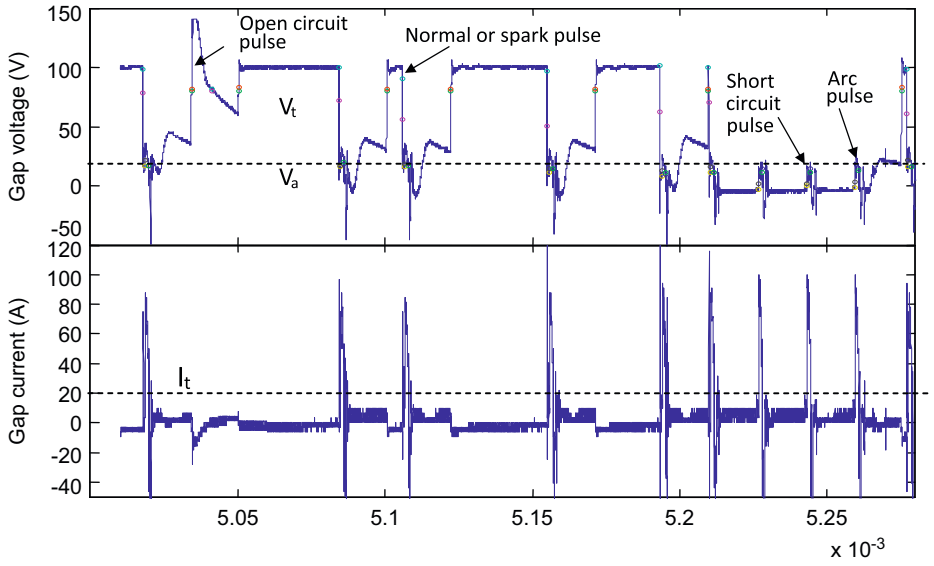

Fig. 3. Pulse train data with different types of discharge pulses.

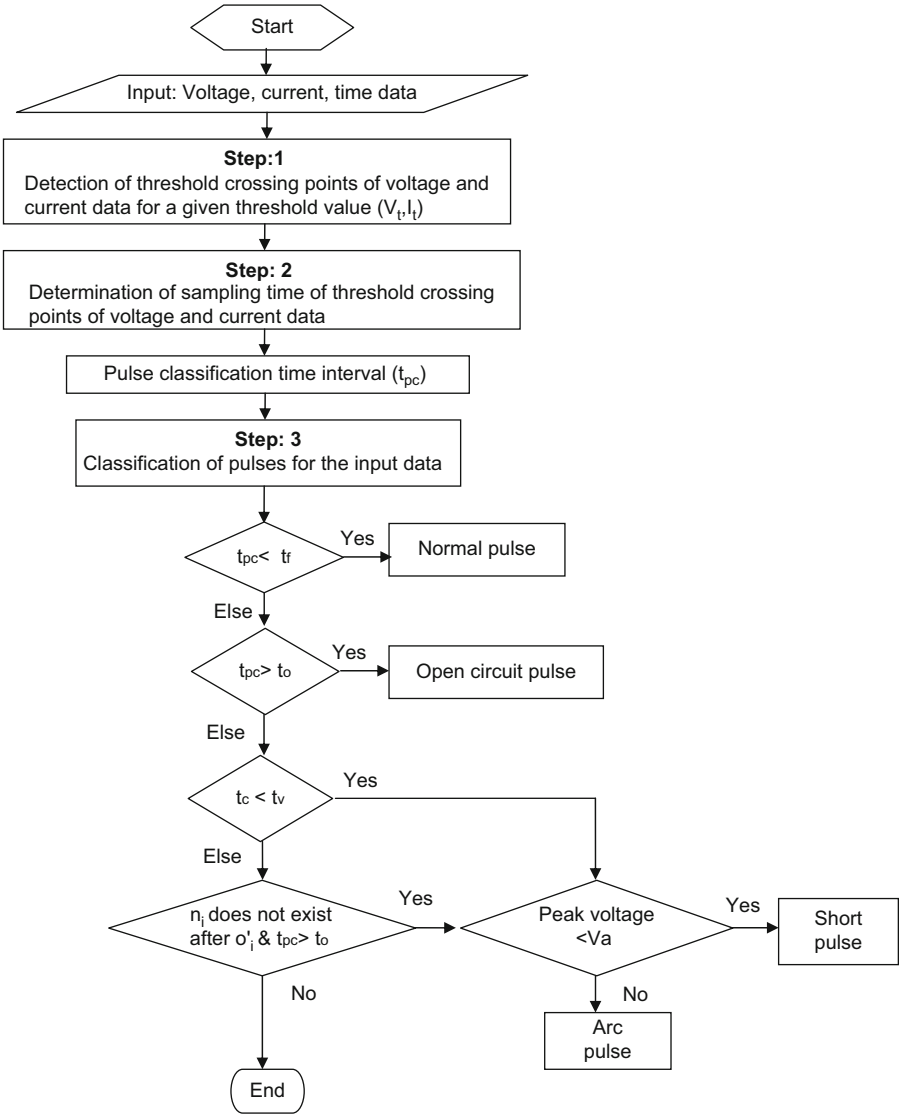

Fig. 4. Flow chart for pulse classification.

3.2. Pulse classification algorithm

The algorithm for classifying pulses is developed based on the detection of threshold crossing points for voltage and current. The flow chart for classifying different types of discharges is shown in Fig. 4. Algorithm for pulse classification has been written using MATLAB and the data obtained is processed using a personal computer. Various steps involved in the proposed algorithm for classifying different types of discharges are explained in this section.

3.2.1. Step 1: Finding the voltage and current threshold crossing points

The voltage, current and time data from the data acquisition system are input to the algorithm. Fig. 5 shows a sample of the gap voltage and current wave from on time scale. A threshold level is given for both voltage (V_t) and current (I_t). Whenever the voltage and current cross the threshold level, the corresponding sampling data point numbers prior to and after the threshold level are stored. The up and down arrows in Fig. 5 indicate the rising and falling directions. The sampling data point numbers crossing the voltage threshold level are stored in matrices **K**, **L** in the rising direction and **M**, **N** in the falling direction. Similarly for the current threshold level crossing points are stored in matrices **O**, **P** and **Q**, **R** as shown in Fig. 5.

3.2.2. Step 2: Detecting voltage, current and time corresponding to threshold level crossing sampling points

The sampling times corresponding to the sampling data points stored in the matrices **K**, **L**, **M**, **N** and **O**, **P**, **Q**, **R** are obtained from the input data. The time corresponding to the sampling data points in matrices **L** and **M** are used to find the average ignition delay time of the pulses.

3.2.3. Step 3: Classification of pulses

The classification of pulses is based on the time interval between the voltage threshold crossing point in the matrix **N** and the corresponding current threshold crossing point in the matrix **O**. n_i represents the voltage threshold crossing point of ith element of the matrix **N**. The time corresponding to n_i is represented as t_v and o_i the current threshold crossing point of the ith element of matrix O. The time corresponding to o_i is represented as t_c. The time difference between t_c and t_v is noted as pulse classification time interval t_{pc} ($t_{pc}=t_c-t_v$).

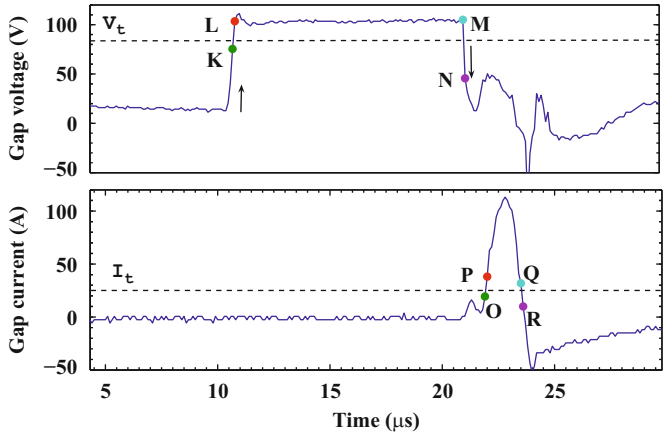

Fig. 5. Detection of voltage and current threshold crossing points for pulse classification.

3.2.3.1. Detection of normal pulse.

In case of normal pulse, current discharge occurs soon after the ignition delay time. The voltage and current threshold crossing points n_i and o_i occur before the discharge completes. Then t_{pc} will be less than discharge duration (t_f) as shown in Fig. 6 ($t_{pc} < t_f$).

3.2.3.2. Detection of open circuit pulse.

In case of open circuit pulses, the current discharge does not occur. Then t_{pc} is calculated with respect to the current threshold crossing point (o_i) of the pulse occurring after the concerned open circuit pulse as shown in Fig. 7. Since the successive pulse occurs only after pulse off time (t_o), t_{pc} should be greater than pulse off time ($t_{pc} > t_o$).

3.2.3.3. Detection of non-ignition delay pulse.

In case of a non-ignition delay pulse ignition delay does not occur and voltage threshold crossing point does not exist. There are two cases in occurrence of non-ignition delay pulse in the input sample data. In the first case, if the non-ignition delay pulse occurs with an ignition delay pulse after it as shown in Fig. 8(a), t_{pc} is calculated with respect to the ignition delay pulse occurring just after the concerned arc pulse. t_{pc} will become negative since $t_c < t_v$ as shown in Fig. 8(a).

In the second case, there is no ignition delay pulse after the corresponding non-ignition delay pulse as shown in Fig. 8(b). In this case t_{pc} is calculated with respect to the voltage threshold crossing point of the ignition delay pulse occurring just earlier to the concerned arc pulse. And $t_{pc} > t_o$ as shown Fig. 8(b).

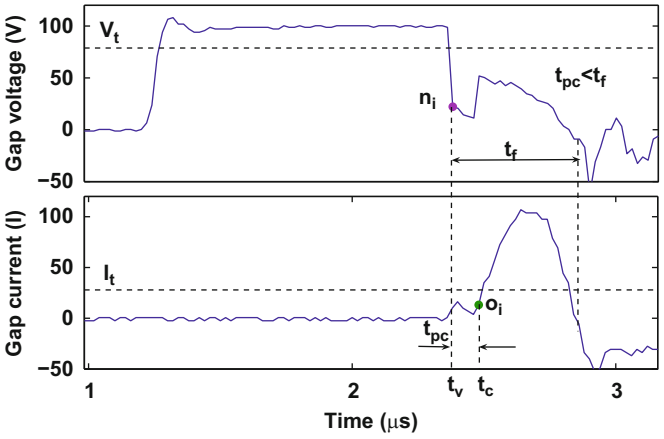

Fig. 6. Detecting normal pulse.

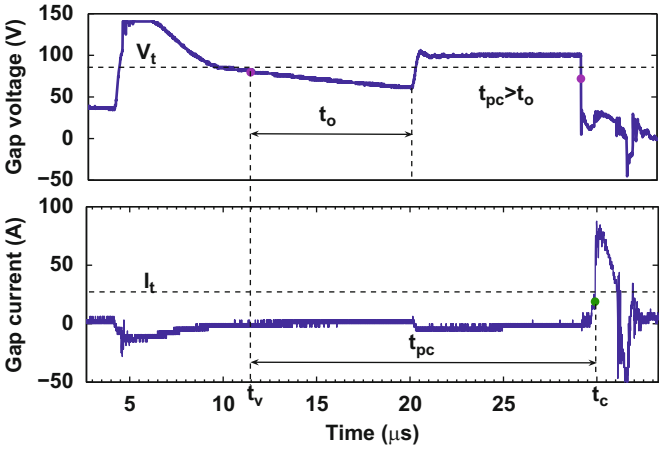

Fig. 7. Detecting open circuit pulse.

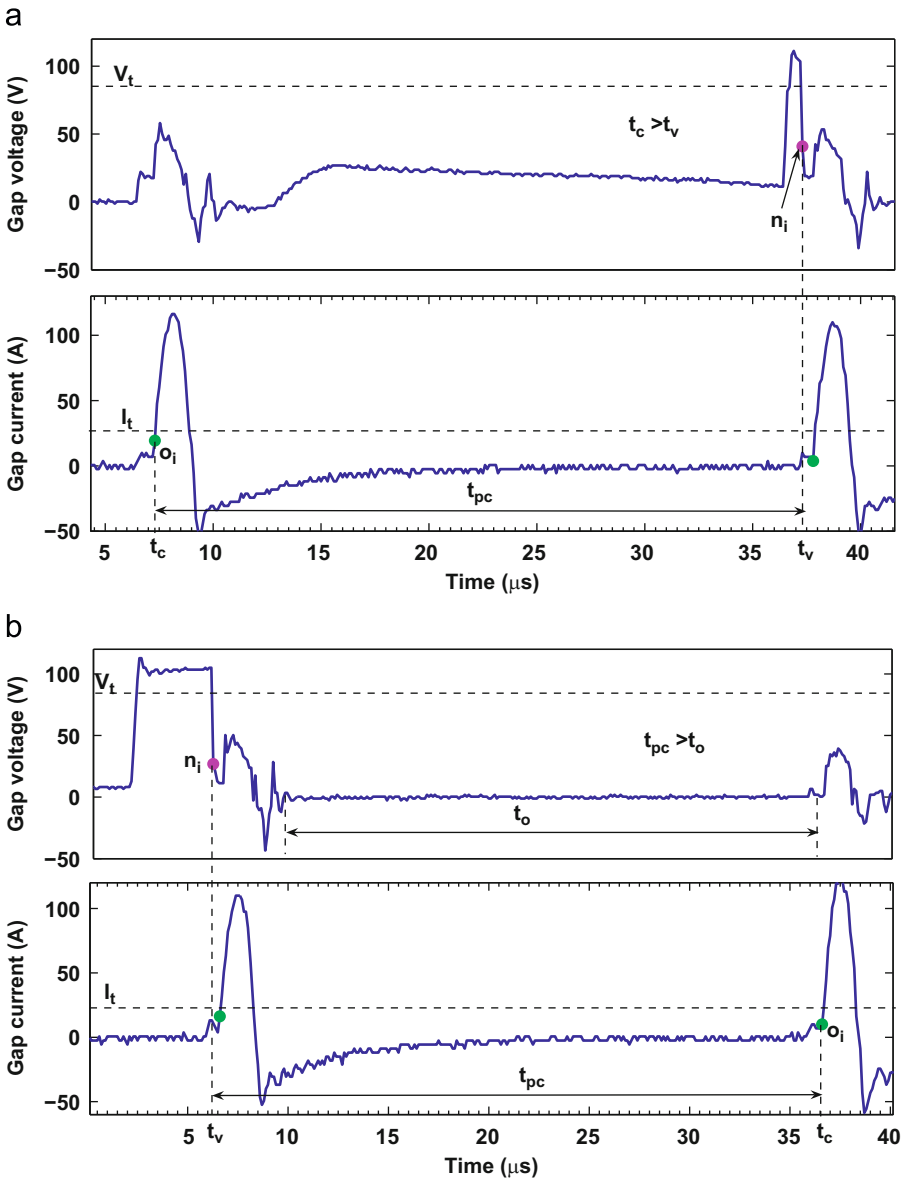

Fig. 8. Detecting non-ignition delay pulse: (a) detecting non-ignition delay pulse (case 1) and (b) detecting non-ignition delay pulse (case 2).

The non-ignition delay pulses are further classified into short and arc pulses. This is done based on the magnitude of their peak voltage. The peak voltage corresponding to a short circuit pulse is less than the arc pulse [18,20]. The threshold voltage (V_a) for classifying different non-ignition delay pulses is taken as 20 V. If the peak voltage of the non-ignition delay pulse is greater than 20 V it is arc pulse and else it is a short circuit pulse.

4. Experiments for WEDT process analysis

The experimental setup for conducting WEDT experiments is shown in Fig. 9. The experiments are conducted on ELECTRONICA ECOCUT WEDM machine. Two sets of experiments are conducted in the present work. In the first set, preliminary experiments are conducted to compare the discharges occurring in WEDM and WEDT to study the variation in discharges occurring when the workpiece is fixed and rotating, respectively .The experiments are conducted on brass material for both WEDT and WEDM. The diameter of the brass workpiece for WEDT is 10 mm, and

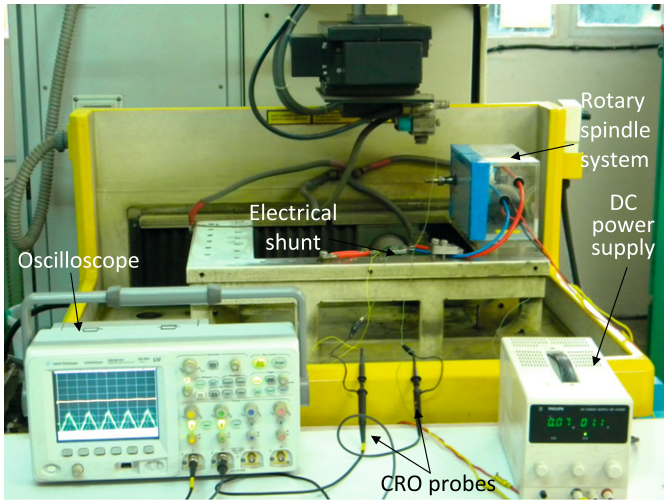

Fig. 9. Experimental setup for WEDT.

thickness of the workpiece for WEDM is 12 mm. The MRR (i.e. volume of the material removed per unit time) is calculated using Eqs. (1) and (2) for WEDT [7] and WEDM [21]. The equation available for mass of the material removed per unit time is modified to get volume of material removed per unit time in WEDM [21]:

$$\text{MRR for WEDT} = \frac{\pi \times (D_1^2 - D_2^2) \times V_f}{4} \quad (1)$$

$$\text{MRR for WEDM} = w \times t \times V_f \quad (2)$$

4.1. Preliminary experiments

Experiments were conducted by varying the pulse off time, for both WEDT and WEDM. The comparison of pulse train graphs at pulse off time 42 μs for WEDT and WEDM is reported in Fig. 11(a) and (b). The arc and normal discharge concentration regions are represented by a rectangular waveform. The peak region represents the arc regions and the valley region represents the normal (spark) discharge region. From Fig. 10 it is observed that at constant pulse off time the number of arcs is more in WEDT than in WEDM. The number of arc regions and width of the arc regions (W_a) are more in WEDT compared to WEDM. The experimental observations made during WEDT and WEDM at different pulse off times are shown in Table 1. It is observed that much fluctuation in the average voltage is observed in WEDT compared to WEDM, which can be attributed to the occurrence of arc regions in WEDT. It is also observed that the MRR in case of WEDT is less than that of WEDM at all the pulse off times. This is due to the increased arc pulses in WEDT, the arc pulses reduce MRR and spark pulses increase MRR [12,19,20]. The possible cause for the occurrence of wider arc regions in WEDT is due to rotation of the workpiece. When discharge occurs, the material is removed from the rotating workpiece and the wire is fed forward during which the unmachined portion of the workpiece faces the wire and the spark gap reduces. This phenomenon increases the formation of arcs and arc regions.

4.2. Experiments to study the effect of machining parameters

The second set of experiments is conducted to study the effect of machining parameters pulse off time, spark gap, servo feed, rotational speed and flushing pressure on MRR, surface roughness and roundness error. The details of the machining parameter settings for the experiments are shown in Table 2. The pulse off times used are 30, 35 and 42 μs. From the preliminary experiments conducted it was observed that for the WEDM machine used the turning process is not consistent at lower pulse off times (below 30 μs). Due to this limitation, aforementioned pulse off times have been chosen. The spark gap and servo feed knobs can be varied from 1 to 10; during this spark gap varies from 10 to 100 μm proportionally. For the present case spark gaps are chosen as 30, 50 and 80 μm since it was observed from preliminary experiments that consistent machining occurred within this range only. Varying the servo feed knob from 1 to

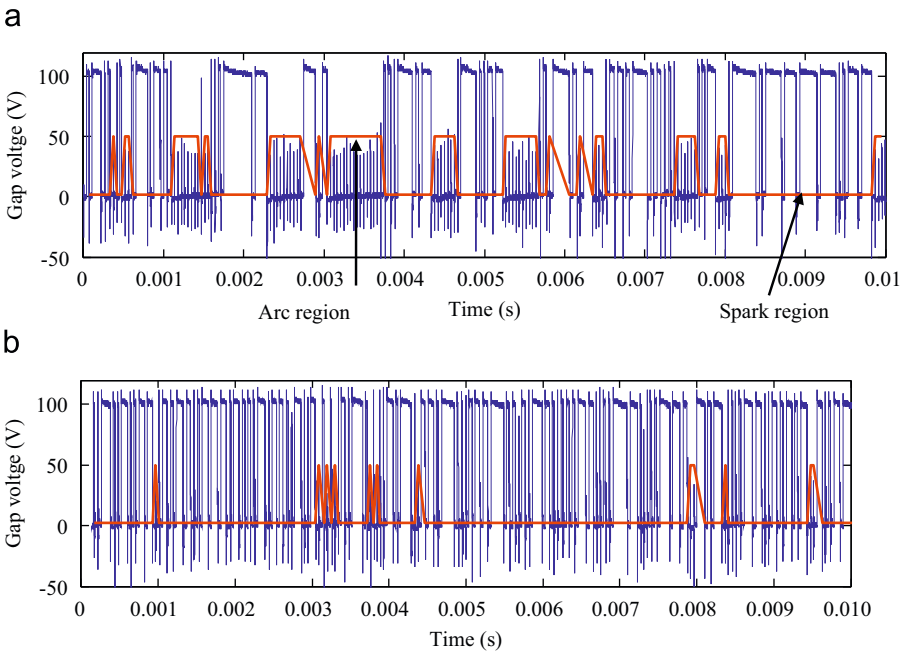

Fig. 10. Comparison of pulse trains for WEDT and WEDM: (a) pulse train data for WEDT representing the arc regions at 42 μs and (b) pulse train data for WEDM representing the arc regions at 42 μs.

Table 1
Observations from preliminary experiments conducted on WEDT.

S. no.	Pulse off time (μs)	Fluctuation in average voltage (V)		Fluctuation in average current (A)		Material removal rate (mm³/min)	
		WEDT	WEDM	WEDT	WEDM	WEDT	WEDM
1	30	44–54	52–56	1.9–2.0	2.0	9.75	15.84
2	35	46–54	50–52	1.4–1.5	1.8	8.67	12.96
3	42	46–52	48–50	0.9–1.0	1.0	6.89	7.68

10 increases the wire federate (Technology manual ECOCUT machine). Servo feed knob is set at 3, 5 and 8 since machining is not consistent below level3 and above level8. Using the worm and helical gear the rotational speed can be varied from 4 to 100 rpm. However at lower rotational speeds helical threads are formed on the workpiece as shown in Fig. 1(c). Because of this the rotational speed is varied between 40 and 100 (40, 70 and 100 rpm). The flushing pressure can be adjusted at three levels using regulating valves. Hence the flushing pressure is chosen as 1 (lower), 2 (medium) and 3 (higher) to cover the total range. The actual values are given in Table 2. The process constants used for conducting experiments are shown in Table 3. The experiments are conducted such that when a particular parameter is varying, all other parameters are kept constant. The constant value used for pulse off time when studying the effect of any other machining parameter is 42 μs. For spark gap and servo feed the constant value is 5. Similarly for rotational speed it is 40 rpm and flushing pressure is set at level 2.

Table 2
Parameter settings for WEDT experiments.

Machining parameter	Parameter levels		
	Level 1	Level 2	Level 3
Pulse off time (μs)	30	35	42
Spark gap (μm)	30	50	80
Servo feed	3	5	8
Flushing pressure (kg/cm^2)	2	4	6
Rotational speed (rpm)	40	70	100

Table 3
Process constants used for WEDT experiments.

Parameter	Value
Wire speed (m/min)	4.0
Depth of cut (mm)	0.3
Diameter of the specimen	10.0
Maching length (mm)	8.0
Material	Brass

5. Results and discussions

The effect of machining parameters on pulse trains, MRR, surface roughness and roundness will be discussed in this section.

5.1. Influence of machining parameters on pulse trains

The pulse train data are collected for a duration of 100 ms at each experimental condition. The results of pulse train analysis with pulse off time, spark gap, servo feed, rotational speed and flushing pressure are shown in Table 4. The number of normal pulses, arc pulses, total number of pulses, average ignition delay time, number of arc regions, width of the arc and normal regions are also shown in Table 4. Open circuit and short circuit pulses did not occur in the data analyzed, so they are represented in Table 4.

5.1.1. Influence of pulse off time

From Table 4, it is observed that the pulse off time has significant influence on the number of arc pulses, total number of pulses and the number of arc regions. With increase in pulse off time from 30 to 42 μs, the number of arc pulses decreased from 945 to 497, the total number of pulses reduced from 1763 to 1219 and the number of arc regions reduced from 159 to 117. Because at higher pulse off times the deionization time available for the charge carriers increases and most of the charge carriers formed during the discharge will get deionized and the flushing available will also be more. Due to this the number of arc pulses reduced from 945 to 497 and arc regions reduced from 159 to 117. Ignition delay time did not vary much with pulse off time.

5.1.2. Influence of spark gap

Spark gap has much influence on most of the pulse train results. From Table 4 it is observed that with increase in spark gap from level 3 to 8, ignition delay time increased from 37 to 160 μs. This is due to the increase in gap resistance. The number of normal and arc discharges reduced from 760 to 430 and from 965

Table 4
Results of pulse train analysis for different machining parameters.

S. no.	Machining parameter	Average number of normal pulses	Average number of arc pulses	Total number of pulses	Average ignition delay time (μs)	Average number of arc regions	Average width of arc region (μs)	Average width of normal discharge region (μs)
1	*Pulse off time*							
	Level 1	818	945	1763	57	150	159	497
	Level 2	812	714	1526	59	145	134	544
	Level 3	722	497	1219	68	128	117	652
2	*Spark gap*							
	Level 1	760	965	1725	37	180	180	371
	Level 2	722	497	1219	67	128	117	652
	Level 3	430	132	562	160	48	70	2033
3	*Servo feed*							
	Level 1	716	447	1164	72	124	100	687
	Level 2	722	497	1219	61	128	117	652
	Level 3	820	545	1365	50	159	111	508
4	*Rotational speed*							
	Level 1	722	497	1219	68	128	117	652
	Level 2	772	487	1259	62	147	94	583
	Level 3	771	590	1361	56	175	99	469
5	*Flushing pressure*							
	Level 1	725	688	1413	57	157	141	491
	Level 2	722	497	1219	68	128	117	652
	Level 3	717	511	1228	68	123	131	677

to 132 with increase in spark gap due to the increase in ignition delay time. At lower spark gap, gap resistance is less and breakdown occurs at a faster rate, and hence the number of discharges per unit time is increased. When the number of discharges increase, the gap contamination will be more and the chances of forming arcs and arc regions increase. Because of this the number of arc regions when the spark gap knob is set at 3 is 180 and at 8 it is 48 as shown in Table 4. The pulse train data collected at different spark gaps is shown in Fig. 11(a)–(c). A reduction in the number of arcs, arc regions, width of the arc region with increase in spark gap can be observed. The width of normal discharge region increases with increase in spark gap since the chances of forming normal discharge are more at higher spark gap.

5.1.3. Influence of servo feed

Increasing the servo feed knob from 3 to 8 increases the wire feed rate (Technology manual ECOCUT). Since it reduces the servo reference voltage, the difference between the average inter-electrode gap voltage and servo reference voltage increases and servo control increases the feed rate [22]. When feed rate increases the gap between the wire and workpiece reduces, leading to the reduction in ignition delay. Due to this the average ignition delay time reduced from 72 to 50 μs with increase in servo feed. The total number of pulses increased from 1164 to 1365 with increase in servo feed level, due to the increase in the number of normal and arc discharges. The average number of normal discharges per unit time increased from 716 to 820 due to reduction in the average ignition delay time. At higher servo feed level since the spark gap reduces due to increased feed rate, the chances of forming arcs increase, because of this the average number of arcs increased from 447 to 545 as shown in Table 4; also the average number of arc regions increased from 124 to 159 with increase in servo feed.

5.1.4. Influence of rotational speed

Rotational speed has significant influence on the number of arc regions. With increase in rotational speed from 40 to 100 rpm, number of arc regions increased from 128 to 175 as shown in Table 4, due to reduction in the spark gap. As the rotational speed increases, the circumferential length of the material crossing the sparking region per unit time increases but the energy input in the form of pulse is the same. So the volume of material removed per unit length or the depth of the material removed at the sparking region reduces. If the depth of material removed is less, the gap between the wire and workpiece decreases. Because of this the chances of forming arcs increases and hence the arc regions increased. A slight reduction in the ignition delay from 68 to 56 μs occurred with increase in rotational speed due to the reduction in the spark gap. For the same reason the total number of discharges increased from 1219 to 1361 as shown in Table 4.

5.1.5. Influence of flushing pressure

Flushing pressure effects the contamination of spark gap with the debris formed. Increasing the flushing pressure flush away the debris formed and gap contamination reduces. It can be observed

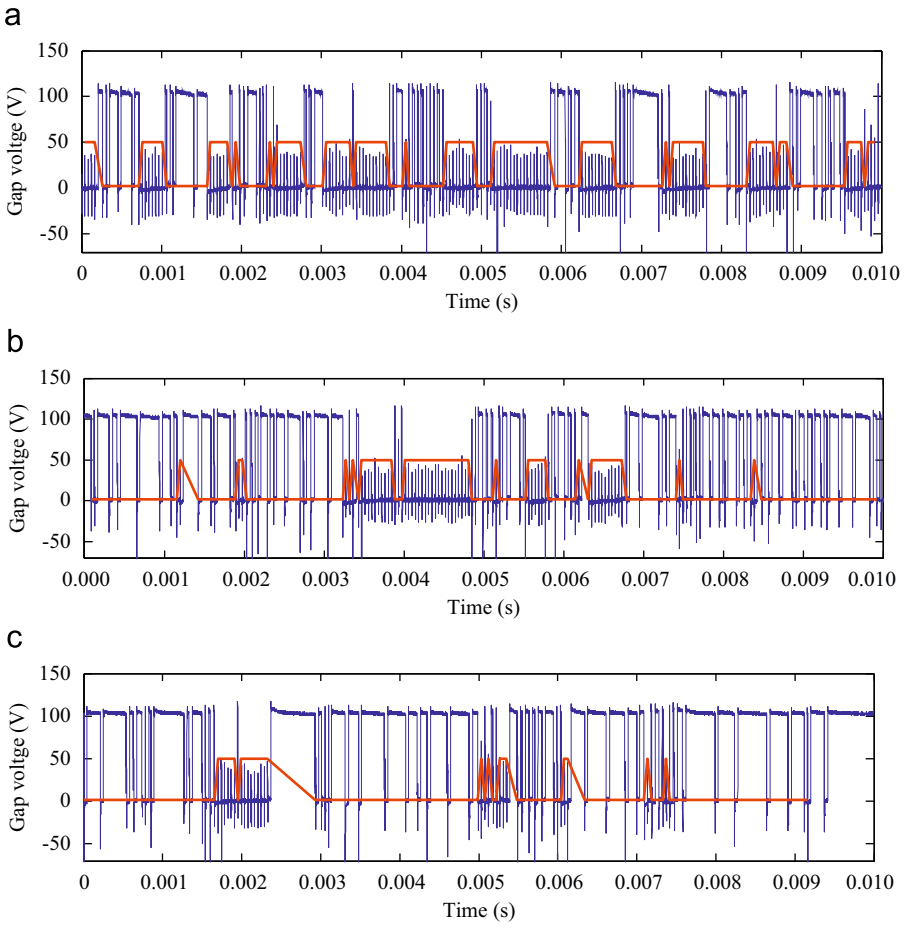

Fig. 11. Variation in pulse trains with spark gap: (a) pulse train data at spark gap 30 μm, normal discharges=63; arcs=112; arc regions=18; Wa=231 μs; Wn=367 μs, (b) pulse train data at spark gap 50 μm, normal discharges=73; arcs=55; arc regions=12; Wa=163 μs; Wn=490 μs and (c) pulse train data at spark gap 80 μm, normal discharges=55; arcs=24; arc regions=8; Wa=95 μs; Wn=715 μs.

Table 5
Experimental results for MRR, roundness error and surface roughness with various machining parameters.

S. no	Machining parameter	Material removal rate (mm^3/min)	Surface roughness		Roundness error (μm)
			Ra (μm)	Rz (μm)	
1	*Pulse off time*				
	Level 1	9.75	4.98	28.98	15.97
	Level 2	8.67	4.35	24.99	12.1
	Level 3	5.89	3.05	19.49	8.61
2	*Spark gap*				
	Level 1	6.75	2.94	17.61	8.91
	Level 2	5.89	3.05	19.63	8.61
	Level 3	3.05	1.56	10.41	6.03
3	*Servo feed*				
	Level 1	5.9	2.6	15.69	8.04
	Level 2	5.89	3.05	19.63	8.25
	Level 3	7.04	3.35	20.53	8.48
4	*Rotational speed*				
	Level 1	5.89	3.05	19.63	8.98
	Level 2	6.84	3.13	19.22	8.21
	Level 3	6.44	2.94	18.32	7.28
5	*Flushing pressure*				
	Level 1	5.94	3.61	21.3	8.91
	Level 2	5.89	3.12	20.1	8.25
	Level 3	6.05	3.18	19.7	7.4

from Table 4 that the flushing pressure shows much influence on the number of arcs and arc regions. When the flushing pressure increased from lower to higher, the number of arcs reduced from 688 to 511 and the arc regions reduced from 157 to 123 due to improved debris condition at spark gap. Flushing pressure did not show considerable variation on the number of normal discharges, it is changed from 725 to 717, which is constant compared to the number of arc discharges.

5.2. Influence of machining parameters on MRR

One of the important parameters that indicate the performance of WEDT process is MRR. The effect of various machining parameters like pulse off time, spark gap, servo feed, rotational speed and flushing pressure on MRR, surface roughness and roundness error is studied and their results are indicated in Table 5.

5.2.1. Influence of pulse off time

Increasing the pulse off time from 30 to 42 μs the MRR changes from 9.75 to 5.89 mm^3/min as shown in Table 5. This can be attributed to the reduction in the total number of discharges per unit time from 1763 to 1219 as shown in Table 4. Since MRR is proportional to the number of discharges and also depends on the type of the discharge [12,19,20].

5.2.2. Influence of spark gap

Spark gap is the parameter that influences the gap resistance. Increasing the spark gap from 30 to 80 μm the MRR is reduced from 6.75 to 3.05 mm^3/min. With increase in spark gap ignition delay time increased from 37 to 160 μs and the total number of discharges per unit time reduced from 1725 to 562 (Table 4), leading to reduction in MRR.

5.2.3. Influence servo feed

Servo feed has less influence on MRR compared to pulse off time and spark gap. Increasing the servo feed setting knob from 3 to 8 increased the MRR from 5.90 to 7.04 mm^3/min as shown in Table 5. This is due to the increase in the number of discharges from 1164 to 1365 as shown in Table 4.

5.2.4. Influence of rotational speed

Increasing the rotational speed from 40–70 rpm MRR increased from 5.89 to 6.84 mm^3/min (shown in Table 5) since the number of normal discharges per unit time increased from 722 to 772. There is a reduction in MRR from 6.84 to 6.44 mm^3/min when the rotational speed is increased from 70 to 100 rpm due to the increase in the number of arcs and arc regions as shown in Table 4.

5.2.5. Influence of flushing pressure

The influence of flushing pressure on MRR is very less compared to other parameters. It has increased from 5.89 to 6.05 mm^3/min as shown in Table 5. This can be attributed to the increase in the number of normal discharges from 725 to 771 and decrease in the number of arc regions from 157 to 123, which is shown in Table 4.

5.3. Influence of machining parameters on surface roughness

Results of varying machining parameters on arithmetic average surface roughness R_a and R_z are represented in Table 5. The surface roughness is measured with a Mahr roughness tester. Roughness is measured at 3 locations along the circumference of WEDT workpiece and their average is represented in Table 5. Surface finish in EDM or WEDM depends on the discharge energy, energy spent per unit time [23] and formation of arc regions and width of the arc region.

5.3.1. Influence of pulse off time

With increase in pulse off time from 30 to 42 μs R_a value reduced from 4.98 to 3.05 μm and R_z value reduced from 28.98 to 19.49 μm as shown in Table 5. This can be attributed to the reduction in the energy per unit time due to the reduction in the number of discharges per unit time 1763–1219 and the reduction in the number of arc regions from 150 to 128 as shown in Table 4.

It is also observed from Table 4 that width of arc region is more at pulse off time 30 μs. Due to this the energy spent is more, forming wide craters, and increases the R_z value since it is calculated based on the maximum peak to peak height of surface roughness profile.

5.3.2. Influence of spark gap

The spark gap has an inverse effect on surface roughness. Increasing the spark gap from 30 to 80 μm decreased R_a from 2.94 to 1.56 μm and R_z from 17.61 to 10.41 μm. This is due to the reduction in the number of discharges and the number of arc regions with increase in spark gap as shown in Table 4. The width of arc region is less at higher spark gap compared to that of the lower one due to this R_z value reduced. At the same time the average ignition delay time increased from 37 to 160 μs; this reduces the energy spent per unit time during normal discharge region and results in reduction of surface roughness.

5.3.3. Influence of servo feed

The surface roughness is directly proportional to servo feed, which is observed from Table 5. Increasing servo feed setting knob from 3 to 8R_a value increased from 2.6 to 3.35 μm and R_z value increased from 15.69 to 20.53 μm. Surface roughness parameters are less at lower servo feed since the servo voltage is high. Due to this the difference between the average inter-electrode gap voltage and servo voltage reduces and the wire feed reduces. This will reduce the chances of forming arcs and arc regions and the number of discharges per unit time also less at lower servo feed than that of the higher one as shown in Table 4, leading to the reduction in energy spent per unit time. The increase in surface roughness parameters with increase in servo feed is due to the increase in the energy per unit time as the number of pulses per unit time and the arc regions are more as shown in Table 4.

5.3.4. Influence of rotational speed

Rotational speed has very less influence on surface roughness. The variation in surface roughness parameters with rotational speed is shown in Table 5. Slight decrease in the R_a and R_z is observed when the rotational speed is increased from 40 to 100 rpm since the circumferential length of the material crossing the spark region per unit time increases about 60%, reducing the energy spent per unit length. Due to this the surface finish of the machined component improved, though there is increase in the number of arc regions as shown in Table 4.

5.3.5. Influence of flushing pressure

Flushing pressure did not show significant effect on the surface roughness parameters. The R_a value decreased from 3.61 to 3.18 μm and the R_z value decreased from 21.30 to 19.70 μm as shown in Table 5. This can be attributed to the reduction in energy due to the reduction in the number of arc regions from 157 to 123 and width of arc regions from 141 to 131 μs. The increase in

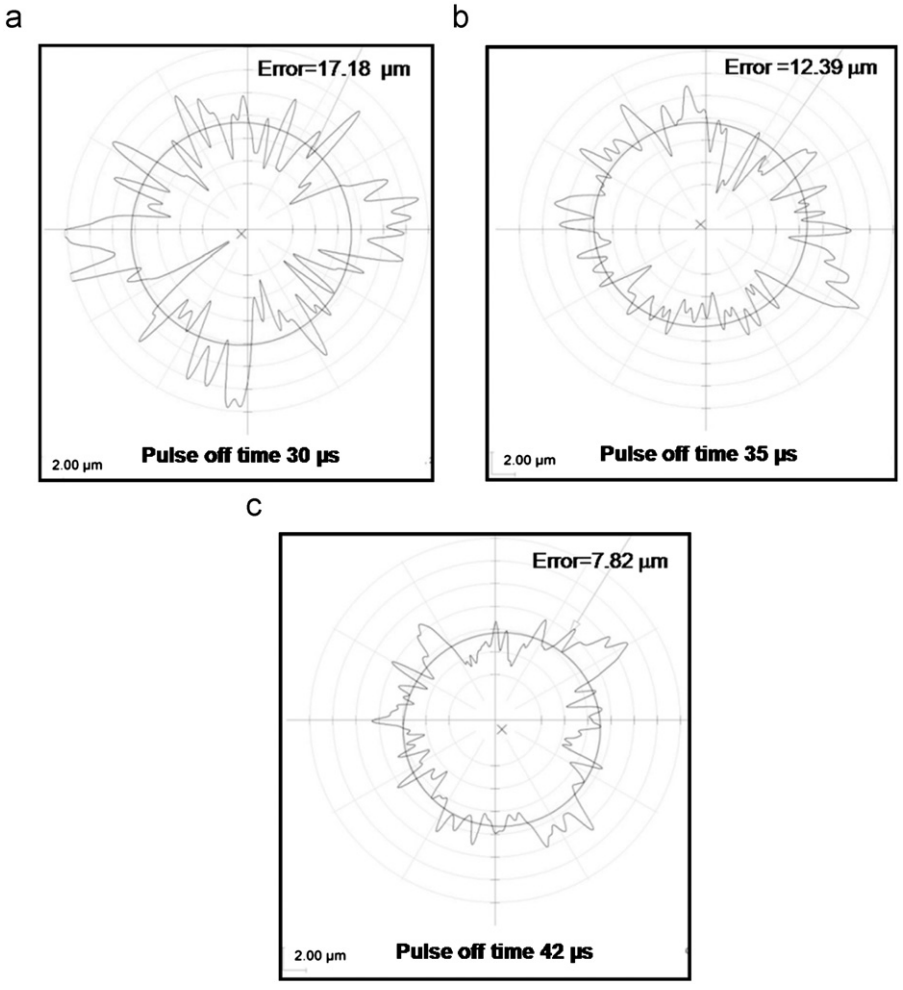

Fig. 12. Roundness profiles at different pulse off times: (a) roundness profile at pulse off time 30 μs, (b) roundness profile at pulse off time 35 μs and (c) roundness profile at pulse off time 42 μs.

average ignition delay time from 57 to 68 μs as seen in Table 4 is also a cause for this.

5.4. Influence of machining parameters on roundness error

Roundness error is measured with the Mahr roundness tester. The roundness is measured at three cross sections of the machined component and their average is shown in Table 5. The maximum peak and valley in the roundness profile depend on the discharge energy per unit time and energy spent per unit length along the circumference of the workpiece. Discharge energy per unit time and length depends on the formation of arc regions, width of the normal and arc regions and the average ignition delay time. A valley may be formed during arc region since the number of discharges per unit time and length along the circumference of the workpiece is more and creates a deep crater. The depth of crater formed during normal discharge region is less compared to that of the arc region. Because the number of discharges per unit time during normal discharge region is less, normal discharge is associated with ignition delay and the energy per unit time reduces and the depth of crater reduces or forms a peak in the roundness profile. The average gap voltage reduces during the arc region, when it is less than the servo voltage, the table is withdrawn and this may also cause an irregularity in the roundness profile. Han et al. [24] mentioned that when the table is withdrawn or wire feed is reduced suddenly, unnecessary streaks are formed, resulting in waviness of the parts machined. The bearing form error also affects the roundness error [8]. The variation in roundness error with various machining parameters is shown in Table 5.

5.4.1. Influence of pulse off time

Pulse off time has an inverse effect on roundness error. Increasing the pulse off time from 30 to 42 μs, the average value of roundness error decreased from 15.97 to 8.61 μm as shown in Table 5. Since the number of discharges per unit time reduces with increase in pulse off time as shown in Table 4, the size of craters formed reduces. Because of this roundness error reduces. The polar plots of roundness profiles collected at different pulse off times are shown in Fig. 12. The roundness profile collected at pulse off time 30 μs is shown in Fig. 12(a). It is observed from Fig. 12(a) that the depth of the valleys is more due to the higher width of the arc regions at pulse off time 30 μs as shown in Table 4. Because of this the roundness error is 17.18 μm, which is more compared to the pulse off times 35 and 42 μs as shown in Fig. 12(b) and (c). As the pulse off time increases, the number of arc regions and width of the arc regions reduced and the width of the normal discharge regions and average ignition delay time increased as shown in Table 4. These result in the reduction of crater size formed and the roundness error reduces as shown in Fig. 12(b) and (c).

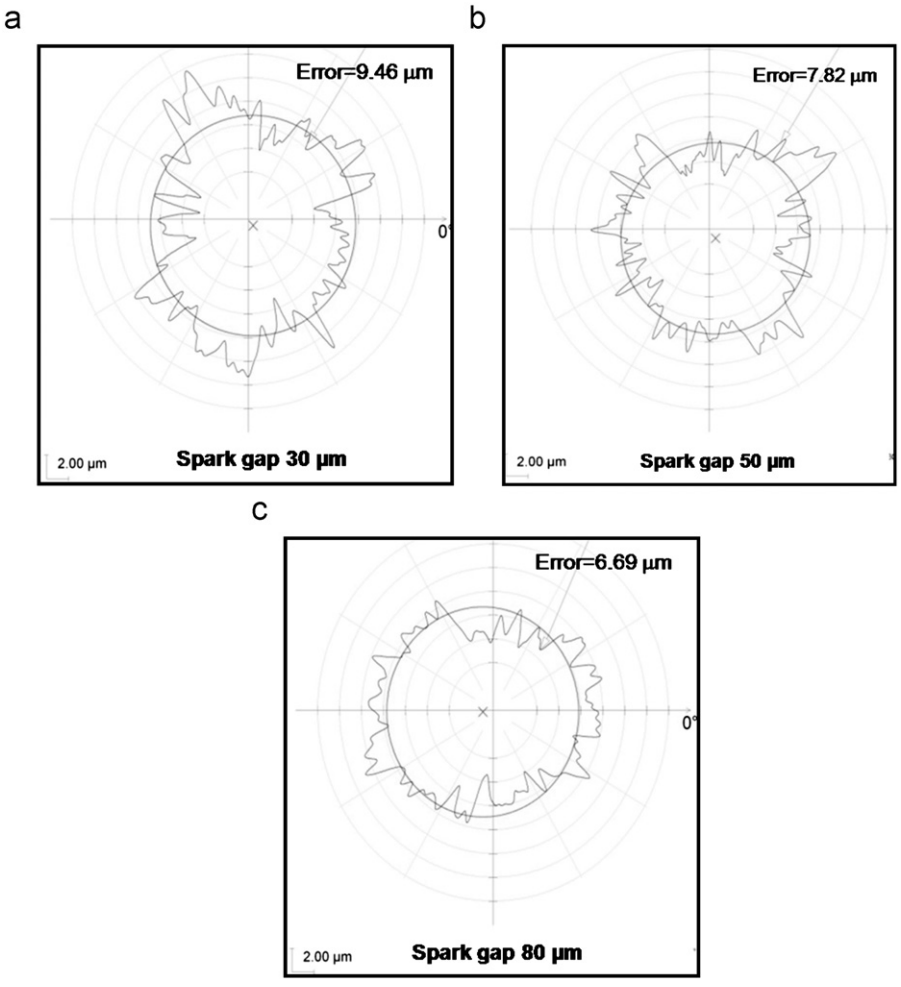

Fig. 13. Variation in roundness profiles with spark gap: (a) Roundness profile at spark gap 30 μm, (b) roundness profile at spark gap 50 μm and (c) roundness profile at spark gap 80 μm.

5.4.2. Influence of spark gap

Increase in the spark gap from 30 to 80 μm reduced the average roundness error from 8.91 to 6.03 μm. Since the energy per unit time reduces as number of discharges, number of arc regions and the width of the arc regions reduce with increase in spark gap as shown in Table 4. The roundness profiles collected at spark gaps are shown in Fig. 13. It is observed from Fig. 13(a) that at spark gap 30 μm the depth of the craters in the roundness profile is more since the average width of the arc regions is more as shown in Table 4. When the spark gap is increased the depth of the craters reduced as shown in Fig. 13(b) and (c). Since at higher spark gap the width of normal regions and ignition delay time increased as represented in Table 4, this will also reduce the energy per unit time and roundness error reduces. The minimum roundness obtained at higher spark is 5.37 μm.

5.4.3. Influence of servo feed

The roundness error increases slightly with increase in servo feed. The roundness error increased from 8.04 to 8.48 μm when the servo feed setting knob is changed from 3 to 8 as shown in Table 5. There is a slight increase in total number of discharges and increase in the average width of the arc regions as shown in Table 4. At the same time a slight reduction in the average ignition delay time also occurred, which will also increase the energy spent during normal discharge region. The number of arc regions increased considerably, which may increase the number of peaks and valleys but will not vary the roundness error since the variation in width of the arc region is less.

5.4.4. Influence of rotational speed

Rotational speed has considerable influence on roundness error. Average roundness error decreased from 8.98 to 7.28 μm. When the rotational speed increases from 40 to 100 rpm the circumferential length of the material crossing the spark region per unit time increases about 60% and hence the roundness error reduced though the number of arc regions increased from 128 to 175 with increase in rotational speed as shown in Table 4. The reduction in the width of the normal and arc regions with increase in rotational speed also contributes to the reduction in roundness error.

5.4.5. Influence of flushing pressure

A slight reduction in the roundness error is observed with increase in flushing pressure as shown in Table 5. This is due to the reduction in the number of arc regions and width of the arc regions with increase in flushing pressure as shown in Table 4. At the same time the average ignition delay time increased, and because of this the energy spent per unit length during the normal discharge region decreases and roundness error reduces.

6. Conclusions

In the present work a precise, simple and cost effective spindle for WEDT process is fabricated. It was observed that the spindle runout is the key parameter affecting consistent machining in WEDT. A data acquisition system for acquiring pulse train data during WEDT process is developed. A pulse classification algorithm for off-line analysis of the WEDT process is developed using MATLAB. Following are the major conclusions from the experimental results:

- Discharge pulses were classified into open circuit, normal, arc and short circuit pulses. The effect of machining parameters on MRR, surface roughness and roundness are analyzed with respect to pulse classification results.
- MRR increased with decrease in pulse off time in both WEDT and WEDM. At a constant pulse off time, MRR in WEDT is less compared to that of WEDM.
- The rotation of workpiece caused arc regions in WEDT process. The number of arc regions and duration of the arc regions observed in WEDT are more than that observed in WEDM.
- MRR is influenced by variation in total number of discharges and the type of discharge. Pulse off time and spark gap have an inverse effect on MRR. Decreasing the pulse off time and spark gap increases the MRR by about 50%. Increasing the servo feed and rotational speed increased the MRR by 17% and 14%, respectively. Flushing pressure has less influence on MRR compared to the other parameters.
- Surface finish improved with decrease in the number of arc regions per unit time and increase in the average ignition delay time. By reducing the pulse off time, the arithmetic average roughness (R_a) reduced by 56% of the total reduction and by reducing the spark gap it has reduced by 43%. Decreasing the servo feed decreased R_a by 22%.
- Roundness error reduced with decrease in the number of arc regions per unit time, increase in the average width of the normal discharge regions and average ignition delay time. By reducing the pulse off time roundness error reduced by 74% and by reducing the spark gap roundness error reduced by 29%. Increasing the rotational speed reduced the roundness error by 17%. Increase in the flushing pressure reduced the roundness error by 15%.

The online control of the process considering the reduction in the number arc regions and control of average ignition delay time as a control strategy can be implemented as a next step to improve the MRR, surface finish and roundness error of the WEDT component.

References

[1] T.A. Spedding, Z.Q. Wang, Study on modeling of wire EDM process, Journal of Materials Processing Technology 69 (1997) (1997) 18–28.
[2] T. Masuzawa, H.K. Tonshoff, Three-dimensional micromachining by machine tools, Annals of the CIRP 46 (1997) (1997) 621–628.
[3] Jun Qu, A.J. Shih, R.O. Scattergood, Development of the cylindrical wire electrical discharge machining process: Part 1: Concept, design, and material removal rate, Journal of Manufacturing Science and Engineering 124 (3) (2002) 702–707.
[4] T. Takayuki, F. Yasushi, M. Naotake, S. Nagao, O Masaaki, Machining phenomena in WEDM of insulating ceramics, Journal of Materials Processing Technology 149 (2004) 124–128.
[5] K. Rhoney, A. Shih, R.O. Scattergood, J. Akemon, D. Gust, M. Grant, Wire electrical discharge machining of metal bond diamond wheels for ceramic grinding, International Journal of Machine Tools and Manufacture 42 (2002) 1355–1362.
[6] A. Mohmmadi, F.T. Alireza, E. Ehsan, K. Davoud, Statistical analysis of wire electrical discharge turning on material removal rate, Journal of Material Processing Technology 205 (2008) 283–289.
[7] M.J. Haddad, A.F. Tehrani, Material removal rate (MRR) study in the cylindrical wire electrical discharge turning (CWEDT) process, Journal of Materials Processing Technology 199 (2008) 369–378.
[8] Jun Qu, A.J. Shih, R.O. Scattergood, Development of the cylindrical wire electrical discharge machining process: Part 2: surface integrity and roundness, Journal of Manufacturing Science and Engineering 124 (3) (2002) 708–714.
[9] M.J. Haddad, A.F. Tehrani, Investigation of cylindrical wire electrical discharge turning (CWEDT) of AISI D3 tool steel based statistical analysis, Journal of Material Processing Technology 198 (2008) 77–85.
[10] A. Mohmmadhi, F.T. Alireza, E. Ehsan, K. Davoud, A new approach to surface roughness and roundness improvement in wire electrical discharge turning based on statistical analysis, International Journal Advanced Manufacturing Technology 39 (2008) 64–73.
[11] F. Han, J. Jiang, D Yu, Influence of discharge current on machined surfaces by thermo analysis in finish cut of WEDM, International Journal of Machine Tools and Manufacture 47 (2007) 1187–1196.

[12] A. Gangadhar, M.S. Shunmugam, P.K. Philip, Pulse train studies in EDM with controlled pulse relaxation, International Journal Machine Tools and Manufacture 32 (5) (1992) 651–657.
[13] D.F. Dauw, R. Snoeys, W. Dekeyser, Advanced pulse discriminating system for EDM process and control, Annals of the CIRP 32 (2) (1983) 541–549.
[14] H Watanabe, T. Wang, I. Suzuki, WEDM monitoring with a statistical pulse classification method, Annals of the CIRP 39 (1) (1990) 175–178.
[15] M.T. Yan, Y.S. Liao, Monitoring and self-learning fuzzy control for wire rupture prevention in wire electrical discharge machining, International Journal of Machine Tools and Manufacture 36 (3) (1996) 339–353.
[16] Y.S. Liao, J.C. Woo, The effects of machining settings on the behavior of pulse trains in the WEDM process, Journal of Materials Processing Technology 71 (3) (1997) 433–439.
[17] Y.S. Tarng, C.M. Tseng, L.K. Chunng, A fuzzy pulse discriminating system for electrical discharge machining, International Journal of Machine Tools and Manufacture 37 (4) (1997) 511–522.
[18] M.T. Yan, H.T. Chien, Monitoring and control of micro wire-EDM process, International Journal of Machine Tools and Manufacture 47 (2007) 148–157.
[19] V.S.R. Murthy, P.K. Philip, Pulse train analysis in ultrasonic assisted EDM, International Journal of Machine Tools and Manufacture 27 (4) (1987) 469–477.
[20] Y.S. Liao, Y.Y. Chu, M.T. Yan, Study of wire breaking process and monitoring of WEDM, International Journal Machine Tools and Manufacture 37 (4) (1997) 555–567.
[21] N. Tosun, Can Cogun, A Gul Tosun, study on kerf width and material removal rate in wire electrical discharge machining based on Taguchi method, Journal of Materials Processing Technology 152 (2004) 316–322.
[22] M.T. Yan, Y.S. Liao, Adaptive control of the WEDM process using the fuzzy control strategy, Journal of Manufacturing Systems 17 (4) (1998) 263–274.
[23] S.H. Lee, X.P. Li, Study on the effect of machining parameters on the machining characteristics in electrical discharge machining of tungsten carbide, Journal of Materials Processing Technology 115 (2001) 344–358.
[24] F. Han, M. Kunieda, T. Sendai and Y. Imai, Simulation of WEDM using discharge location searching algorithm. In: Proceedings of the 10th International Conference on Precision Engineering (ICPE), July 18–20, 2001, Yokohama, Japan, pp. 319–323.